The published paper is available at
Chemical Physics Letters, 568–569 (2013) 59–62.

Kinetics and mechanism of the reaction of acetonyl radical, $CH_3C(O)CH_2$, with Br_2

Gábor L. Zügner, Emese Szabó, Mária Farkas, Sándor Dóbé*

Institute of Materials and Environmental Chemistry, Research Centre for Natural Sciences, Hungarian Academy of Sciences, Pusztaszeri út 59-67, H-1025 Budapest, Hungary

Katarzyna Brudnik*, Dariusz Sarzyński, Jerzy T. Jodkowski[1]

Department of Physical Chemistry, Wroclaw Medical University, 50-140 Wroclaw, pl. Nankiera 1, Poland

Supplementary information associated with this article is available online at
http://dx.doi.org/10.1016/j.cplett.2013.03.026

*Corresponding authors. *E-mail*: dobe.sandor@ttk.mta.hu (S.D.); katarzyna.brudnik@umed.wroc.pl (K.B.).
[1]Deceased.

Kinetics and mechanism of the reaction of acetonyl radical, $CH_3C(O)CH_2$, with Br_2

Gábor L. Zügner, Emese Szabó, Mária Farkas, Sándor Dóbé[*]

Institute of Materials and Environmental Chemistry, Research Centre for Natural Sciences, Hungarian Academy of Sciences, Pusztaszeri út 59-67, H-1025 Budapest, Hungary

Katarzyna Brudnik[*], Dariusz Sarzyński, Jerzy T. Jodkowski[2]

Department of Physical Chemistry, Wroclaw Medical University, 50-140 Wroclaw, pl. Nankiera 1, Poland

Abstract

The low pressure fast discharge flow method with laser induced fluorescence detection of $CH_3C(O)CH_2$ was employed to study the kinetics of the reaction $CH_3C(O)CH_2 + Br_2 \rightarrow CH_3C(O)CH_2Br + Br$ (1) at 298, 323 and 365 K. The rate coefficient at room temperature is $k_1 = (2.33 \pm 0.04\ (2\sigma)) \times 10^{-12}$ cm^3 molecule^{-1} s^{-1}, which increases slightly with increasing temperature. Quantum chemistry (G2) and theoretical rate theory (conventional TST) computations have supplied results in qualitative agreement with experiment. The relatively slow rate of reaction (1) can be due to the resonance stabilization of the acetonyl radical.

Keywords: reaction kinetics, acetonyl radical, Br_2 molecule, resonance stabilization

1. Introduction

Acetonyl (1-methylvinoxyl) radical, $CH_3C(O)CH_2$, plays an important role in the chemistry of the troposphere affecting HOx and NOx cycles and in this way tropospheric O_3 budget. Acetonyl is formed via hydrogen abstraction reactions by OH radicals and Cl atoms from acetone, which is one of the most abundant organics in the background troposphere [1]. Beside its importance for atmospheric chemistry, acetonyl radical is of interest from a fundamental chemical kinetic point of view as well. The radical site in acetonyl is partially delocalized over the carbonyl double bond, which has been found to give rise to unusual kinetic behavior in some of the elementary reactions of this free radical [2,3]. As a continuation of our previous experimental and theoretical work [2-4] on the structure-reactivity relations of acetonyl, we have studied the reaction of $CH_3C(O)CH_2$ radical with Br_2

[*]Corresponding authors. *E-mail*: dobe.sandor@ttk.mta.hu (S.D.); katarzyna.brudnik@umed.wroc.pl (K.B.).
[2]Deceased.

molecule (1). This reaction has relevance also for the enthalpy of formation of the acetonyl radical: in the classical photobromination study of acetone by King et al [5], reaction (1) was assumed to have small positive activation energy at deriving $\Delta_f H°_{298}$ ($CH_3C(O)CH_2$), but no method was available at the time of the investigations to confirm the assumption of the authors.

We have applied the direct reaction kinetic method of low pressure fast discharge flow (DF) coupled with laser induced fluorescence (LIF) monitoring of $CH_3C(O)CH_2$ to determine rate coefficients for reaction (1) at a few temperatures. Preliminary quantum chemical and theoretical reaction kinetic computations have been carried out to interpret and supplement the experiments. The enthalpy of formation of the $CH_3C(O)CH_2Br$ molecule has also been estimated by theory.

To our knowledge, no experimental or theoretical study has been reported on the reaction of acetonyl with Br_2:

$$CH_3C(O)CH_2 + Br_2 \rightarrow CH_3C(O)CH_2Br + Br \qquad (1)$$

2. Methods

2.1 Experimental

The applied DF–LIF technique has recently been described in detail [2] and hence only a brief summary is given here.

The flow reactor was a 40.3 mm i.d. Pyrex tube which was equipped with a coaxially mounted moveable quartz injector to vary the reaction time. A thermostatting jacket surrounded the reactor through which temperature regulated distilled water was flown. $CH_3C(O)CH_2$ radicals were produced in the injector by reacting acetone with F atoms obtained from microwave dissociation of F_2. Br_2 /He gas mixture was introduced at the upper end of the reactor through a side arm. In order to diminish the wall loss of acetonyl, the inner surface of the reactor was coated with Halocarbon Wax (HW). The reaction was monitored by LIF detection of the depletion of the concentration of $CH_3C(O)CH_2$ along the reaction distance. For excitation, we have used the third-harmonic generation wavelength (355 nm) of a Nd:YAG laser. That is, we have made use of our recent findings that the acetonyl radical can be detected with good sensitivity not only by a tunable laser source but also using a fixed-wavelength Nd:YAG laser [2]. The pulsed LIF radiation emerging from the detection

volume was passed through a 436 ± 25 nm band-pass filter, captured by a photomultiplier and averaged with a digital storage oscilloscope.

Helium (Linde, 99.996%) was the carrier gas which was passed through liquid-nitrogen-cooled traps before entering the flow system. F_2 (5% in 99.9995% He) was supplied by Messer-Griesheim. Acetone (Aldrich, 99.9+% HPLC grade) was degassed by freeze (77 K)–pump–thaw cycles in a vacuum line. Br_2 (Sigma-Aldrich, > 99.5+%) was subjected to repeated low temperature vacuum distillations prior to use. HW was purchased from Halocarbon Products Corporation.

2.2 Theoretical method

Ab initio quantum chemical computations were performed in order to locate and characterize the relevant stationary points of the potential energy surface (PES) of the reaction. All equilibrium and transition-state (TS) structures were fully optimized at both the SCF and MP2 levels using the 6-31G(d) basis set. The Gaussian-2 (G2) composite method was used to compute the energies of all species and of the transition state. The method carries out geometry optimization and a subsequent frequency calculation at SCF/6-31G(d), followed by a second geometry optimization at MP2 with the same basis set [6]. The minimal energy pathways were determined by intrinsic reaction coordinate analysis (IRC) at the SCF/6-31G(d) level of theory [6].

Transition state theory (TST) in its conventional formulation was applied to obtain rate constants for the studied reaction by making use of the computed ab initio data. The vibrational and rotational contributions to the thermodynamic functions were derived by the RRHO approximation (no free or internal rotation was considered). The tunneling correction factor was estimated by using the Wigner's formula. [7]

3. Results and discussion

3.1 Experimental rate coefficient

The conventional "on-off" pseudo-first-order experiments and evaluation procedure [8] were applied with $[Br_2] >> [CH_3C(O)CH_2]_0 \approx 4 \times 10^{11}$ molecule cm^{-3} to determine the rate coefficient, k_1, for the overall reaction between acetonyl and Br_2. Under pseudo-first-order conditions, the exponential decay constant, $k_1' = k_1 [Br_2]$, can be obtained from the expression

$-\ln(S_{on}^{Ac}/S_{off}^{Ac}) = k_1' (z/w) = k_1' t$, where S_{on}^{Ac} and S_{off}^{Ac} are the LIF signal strengths of the acetonyl radical in the presence and absence of Br_2, respectively, z is the varied reaction distance, w is the linear flow velocity and t is the reaction time. From k_1', the bimolecular rate coefficient is obtained by varying $[Br_2]$.

Representative pseudo-first-order $CH_3C(O)CH_2$ decays at 322 K are presented as semilogarithmic plots in the inset of Fig. 1, and k_1' vs. $[Br_2]$ data are plotted for the same temperature in the main panel. The linearity and zero intercepts of the pseudo-first-order plots indicate that reaction (1) was studied under kinetically isolated conditions; k_1' and k_1 have been obtained by linear least squares analysis. The pseudo-first-order kinetics were obeyed well at 298 and 361 K reaction temperatures too. The ln S_{off}^{Ac} data as a function of reaction time gave also straight lines, their slopes provided $k_{wall} = (9 \pm 5)$ s^{-1} rate coefficient for the heterogeneous wall loss of acetonyl independent of temperature. The errors given throughout the Letter refer to 2σ precision if not otherwise stated. The experimental conditions and results are compiled in Table 1.

To the best of our knowledge, the rate coefficients presented in Table 1 are the first determinations for the reaction of $CH_3C(O)CH_2$ with Br_2. Up to now, we have performed kinetic experiments only at three temperatures over the limited range of T = 298–361 K. Nevertheless, the data determined are believed to be sufficiently accurate to conclude that the rate of reaction (1) slightly, but definitely increases with increasing temperature. The temperature dependence corresponds to the Arrhenius activation energy of $E_{A,1} \approx 2.3$ kJ mol^{-1}. Clearly, experiments at more temperatures and in a wider range are needed to determine the accurate temperature dependence of reaction (1).

Table 1

Experimental conditions and kinetic results for the reaction $CH_3C(O)CH_2 + Br_2$ (1) [a]

T (K)	P (mbar)	w (cm s^{-1})	10^{-13} $[Br_2]$ (molecule cm^{-3})	k_1' (s^{-1})	10^{12} ($k_1 \pm 2\sigma$) (cm^3 $molecule^{-1}$ s^{-1})	No. of expts
298 ± 3	3.5 ± 0.6	1070	0.5–11.9	19.8–279	2.33 ± 0.04	14
322 ± 2	3.5 ± 0.2	1230	0.25–8.7	11.5–233	2.53 ± 0.16	8
361 ± 2	3.4 ± 0.2	1300	0.42–6.5	12.4–185	2.73 ± 0.06	7

[a] Results of the individual experiments are available as Supplementary data.

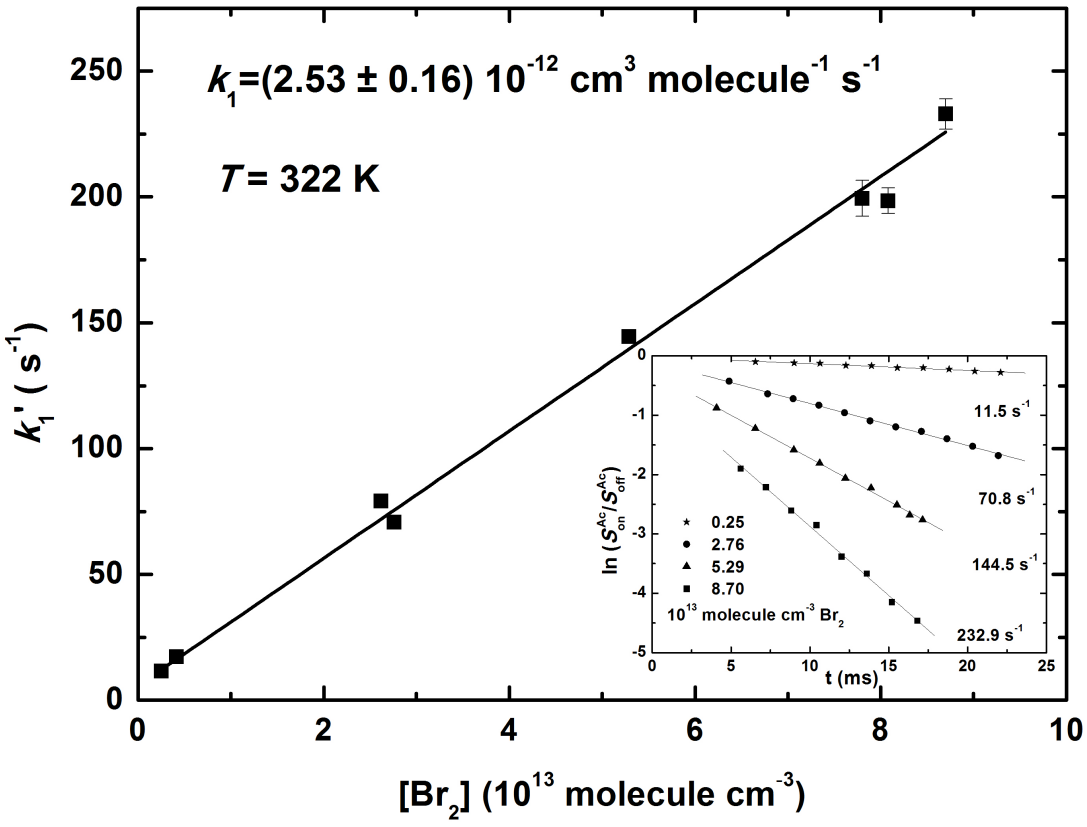

Figure 1. Representative pseudo-first-order plot (main panel) and acetonyl LIF decays (inset) determined for the $CH_3C(O)CH_2$ + Br_2 (1) reaction at T = 322 K.

3.2 Theoretical results

Schematics of structural features and the zero-point energy corrected relative energies computed for the $CH_3C(O)CH_2 + Br_2$ (1) reaction are summarized in Fig. 2 (numerical values of geometrical parameters, frequencies and G2 energies are available as Supporting data). The reaction has been found to occur through a pre-reaction $CH_3C(O)CH_2$…Br–Br complex (van der Waals adduct, MC) formed barrierless from the reactants. The pre-reaction complex has a loosely bound cyclic structure with H…Br distances greater than 3 Å and it is stabilized by just 5.4 kJ mol^{-1} binding energy (at 0 K, with respect to reactants). It is noted that the basis set superposition error (BSSE) can be significant for such a loose complex at the theoretical level and basis set applied; no correction for BSSE [9] has been made in the current work. The minimum energy pathway connects the complex and the products, $CH_3C(O)CH_2Br + Br$, through a transition-state structure (TS) having one imaginary frequency (first order saddle point). A small barrier height of 1.0 kJ mol^{-1} above reactants has been predicted for the TS at the G2 theoretical level. No post-reaction complex between the products could be located on the PES.

Reaction (1), the methathesis reaction between acetonyl and Br_2, is significantly exothermic, indicating that the weak Br–Br bond is replaced by a stronger C–Br bond: the computed G2 reaction enthalpy is $\Delta_r H°_{298}$ (1) = –73.1 kJ mol^{-1} (it is –73.3 kJ mol^{-1} at T = 0 K). The value of $\Delta_r H°_{298}$ (1) = –64.9 ± 8.5 kJ mol^{-1} can be obtained by taking the standard enthalpies of formation of $CH_3C(O)CH_2$, Br_2 and Br from a recent critical data evaluation [10] as well as $\Delta_f H°_{298}$ ($CH_3C(O)CH_2Br$) from [11]. Theory overestimates the exothermicity of the reaction by ~8 kJ mol^{-1}, but this is still a reasonable agreement in view of the significant uncertainty of the literature reaction enthalpy (the errors given are propagated values).

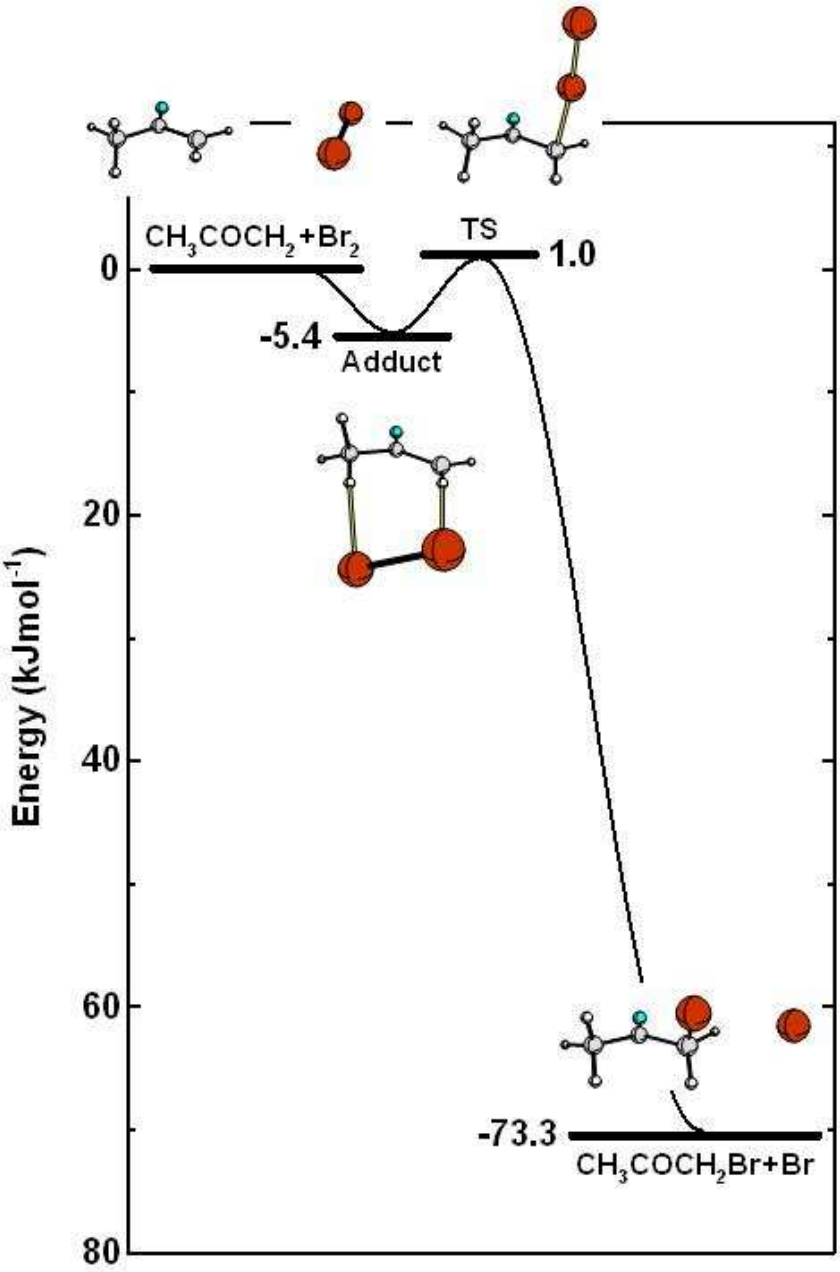

Figure 2. Profile of the potential energy surface and molecular structures for the reaction $CH_3C(O)CH_2 + Br_2$ (1). The energies given have been computed at the G2 level of theory (T = 0 K) and include the MP2/6-31G(d) zero-point energy corrections. Drawings of the molecular structures are based on MP2/6-31G(d) optimization.

The G2 molecular parameters and energies have been applied in conventional TST analysis to calculate rate coefficient for reaction (1); the activation barrier was taken relative to reactants, E_0 = 1 kJ mol^{-1} (T = 0 K). That is, we have assumed the pre-reaction acetonyl…Br_2 complex to have no kinetic effect: the system flies over the shallow potential well without being reverted to reactants or stabilized by collisions. The imaginary frequency obtained at the SCF/6-31G(d) theoretical level is –284 cm^{-1} (not scaled) which corresponds to 8% and 5% Wigner's tunneling corrections at 298 and 361 K, respectively (details of the kinetic calculations are presented as Supporting data). The small tunneling effect is in accordance with that the reaction involves the abstraction of a heavy bromine atom. The calculated rate coefficients increase with increasing temperature and can be represented by the equation of k_1(TST) = 2.7 × 10^{-13} (T/300)$^{2.1}$ cm^3 molecule^{-1} s^{-1}. The computed and measured rate coefficients are compared at a few temperatures in Table 2.

Table 2

Comparison of rate coefficients obtained by DF-LIF experiments and G2/TST computations given in 10^{-12} cm^3 molecule^{-1} s^{-1}

Temperature (K)	200	298	322	361	500	1000
k_1(theory)	0.12	0.26	0.31	0.40	0.81	3.80
k_1(experiment)	-	2.33	2.53	2.73	-	-

As seen in Table 2, theory predicts a small positive temperature dependence similarly to the experimental findings, but the absolute values of the theoretical rate coefficients are on average ~8-times smaller. A potential problem is that single-reference electron correlation method has been used for describing the system with electron delocalization. Also, the acetonyl…Br_2 pre-reaction complex should be characterized at a higher level of theory with more extended basis set and then attempted its kinetic role to be assessed by relevant rate theories, such as the 2TS-model [12], [13], or the statistical adiabatic channel model / RRKM approach [14].

As far as we know, CH_3 + Br_2 is the only polyatomic free radical + Br_2 reaction that has been the subject of quantum chemical and theoretical reaction kinetic investigations [15]. Drougas and co-workers have studied this reaction at the CCSD(T)//MP2/6-31+G(d,p) theoretical level and performed extended RRKM theory and quasi-classical trajectory (QCT) computations [15]. They have found the CH_3 + Br_2 reaction to proceed through a shallow

pre-reaction complex (with ~4 kJ mol^{-1} stabilization energy) in the entrance channel, followed by a low barrier (~1 kJ mol^{-1}) transition state structure, but unlike in our case, they have also mapped a post-reaction complex, $CH_3Br…Br$, in the exit channel formed with a substantial amount of excess energy [15]. The microcanonical RRKM and QCT computations have supplied rate coefficients in good agreement with experiment [16].

3.3 Reactivity of the acetonyl radical

Acetonyl has a partially delocalized electronic structure that may be portrayed by the limiting "alkyl", $•CH_2C(=O)CH_3$, and "alkoxyl", $CH_2=C(–O•)CH_3$, resonance structures [17], [18]. The current experimental and theoretical study confirms our previous conclusion [2-4] that acetonyl reacts like a carbon-centered free radical and not like an alkoxyl radical in its elementary reactions. Specifically, $BrCH_2C(=O)CH_3$ is formed in the reaction with Br_2, while alkoxyl radicals apparently do not enter reaction with molecular bromine [19].

The reaction of acetonyl radical with molecular bromine is quite fast, but it is much slower compared with the alkyl radical + Br_2 reactions [16]; for example, the room temperature rate coefficient is ~50-times smaller than that of the C_2H_5 + Br_2 reaction (Table 3). The reduced reactivity can be attributed to the delocalized electronic structure of the acetonyl radical that has been observed also for the $CH_3C(O)CH_2$ + O_2 [2,3] and $CH_3C(O)CH_2$ + NO reactions [2-4]. A measure of the electron delocalization is the resonance stabilization energy (RSE), which is 23 kJ mol^{-1} for the acetonyl radical [10]; the "prototypical" resonance-stabilized $CH_2=CHCH_2$ (allyl) and $HC≡CCH_2$ (propargyl) radicals have 60 and 39 kJ mol^{-1} RSE, respectively [10], [20].

Timonen and co-workers have studied the kinetics of the reactions of a great number of carbon-centered free radicals with Br_2 using the pulsed laser photolysis technique coupled with time-resolved photoionization mass spectrometry detection [16], [21], [22], [23]. They have established, among several other kinetic features, that resonance stabilized unsaturated hydrocarbon radicals (allyl and propargyl) have significantly lower reactivity toward Br_2 than their saturated counterparts without resonance stabilization [22]. On the other hand, a higher RSE value of the free radical does not mean that it would necessarily react with a smaller rate coefficient [22]. These conclusions are in line with our results concerning the reactivity of the $CH_3C(O)CH_2$ radical with Br_2 (rate coefficients of the Br_2-reactions at T = 298 K are compared in Table 3).

Table 3

Comparison of room temperature rate coefficients of the reactions of selected organic free radicals with molecular bromine

Radical, R	k(R + Br_2, 298 K) (cm^3 $molecule^{-1}$ s^{-1})	RSE (R)[a] (kJ mol^{-1})
CH_3 (methyl)	3.6×10^{-11} [16]	0
CH_3CH_2 (ethyl)	1.1×10^{-10} [16]	0
HCO (formyl)	7.2×10^{-11} [21]	0
CH_2=$CHCH_2$ (allyl)	9.3×10^{-12} [22]	60 [10]
HC≡CCH_2 (propargyl)	1.2×10^{-12} [22]	39 [10] [20]
$CH_3(CO)CH_2$ (acetonyl)	2.3×10^{-12} This work	23 [10]
CH_3O (methoxy)	$< 8 \times 10^{-16}$ [19]	0

[a] Resonance stabilization energies defined as RSE(allyl) = D$H°_{298}$ (H–$CH_2CH_2CH_3$) – D$H°_{298}$ (H–CH_2CH=CH_2), RSE(propargyl) = D$H°_{298}$ (H–$CH_2CH_2CH_3$) – D$H°_{298}$(H–CH_2C≡CH) and RSE(acetonyl) = D$H°_{298}$ (H–$CH_2CH_2CH_3$) – D$H°_{298}$ (H–$CH_2C(O)CH_3$) differences of bond dissociation energies. Zero RSE means that the given free radical has no electron delocalization.

3.4 Thermochemical implications

The long established standard enthalpy of formation of acetonyl, $\Delta_f H°_{298}$ ($CH_3C(O)CH_2$) = –23 ± 8 kJ mol^{-1}, was proposed by King et al. by kinetic study of the gas-phase bromination of acetone [5], while the recent reports converge to a value which is ~10 kJ mol^{-1} smaller (a thorough overview of the literature has been presented in [18]). The critically evaluated, recommended value is $\Delta_f H°_{298}$ ($CH_3C(O)CH_2$) = –34 ± 3 kJ mol^{-1} [10].

King and co-workers [5] measured the initial rates of the consumption of Br_2 in the temperature range 494–618 K using spectrophotometric techniques, and derived kinetic parameters for the elementary reaction Br + $CH_3C(O)CH_3$ ↔ $CH_3C(O)CH_2$ + HBr from which the $\Delta_f H°_{298}$ ($CH_3C(O)CH_2$) value given above was obtained. The derivation was based

on a simple reaction mechanism, including $CH_3C(O)CH_2$ + Br_2 (1), and an assumed activation energy of E_1 = 4 ± 4 kJ mol^{-1} for this reaction. The activation energy we have estimated by direct kinetic experiments is $E_1 \approx$ 2.3 kJ mol^{-1}, which basically confirms the assumption of King et al. [5]. Therefore, we have re-evaluated the standard enthalpy of formation of acetonyl by taking the experimental data of these authors and making use of our E_1 and auxiliary thermochemical data from recent sources[10], [24], [25], [26]. The re-calculation has returned –23 kJ mol^{-1} for $\Delta_f H°_{298}$ (CH_3COCH_2), that is, the very same value as reported by King et al. [5]. Obviously, it does not follow from this analysis that the 'old' enthalpy value should be preferred. In fact, currently there has been a clear consensus in favor of the lower enthalpy of formation of acetonyl [10], [18] as noted. Some systematic errors may have occurred in the experiments of King and co-workers [5], or some of the assumptions they made were not correct to evaluating the experimental data. For example, termination of Br-atoms may have occurred on the walls of the reactor and so their steady state concentration was no longer controlled by the thermodynamic equilibrium in the homogeneous gas phase as assumed by King et al. [5].

In the reaction of acetonyl with Br_2, bromoacetone (acetonylbromide) and Br are the reaction products. Bromoacetone is formed also in the atmospheric degradation of 1-bromopropane [27] and it is one of the marker molecules for Br-atoms during the tropospheric ozone depletion episodes in the Arctic [28]. The only value for the enthalpy of formation of bromoacetone has been reported also by King and co-workers from an experimental study similar to that discussed in the previous paragraph proposing $\Delta_f H°_{298}$ ($CH_3C(O)CH_2Br$) = –180 ± 8 kJ mol^{-1} [11]. In our current work we have applied the G2 theoretical method with the atomization approach [6] to estimate a value of –170.2 kJ mol^{-1} for the standard enthalpy of formation of $CH_3C(O)CH_2Br$. In the absence of other information, the average of the two data is proposed to be used as a compromise, but given with a large uncertainty: $\Delta_f H°_{298}$ ($CH_3C(O)CH_2Br$) = –176 ± 8 kJ mol^{-1}.

Acknowledgements

This work has been supported by the Hungarian Research Fund OTKA (contract OMFB-00992/2009) and the Polish-Hungarian Academic Exchange Program (No. 21 / 2011).

Supplementary data

Supplementary data associated with this article can be found in the online version at http://...

References

[1] H.B. Singh, L.J. Salas, R.B. Chatfield, E. Czech, A. Fried, J. Walega, M.J. Evans, B.D. Field, D.J. Jacob, D. Blake, B. Heikes, R. Talbot, G. Sachse, J.H. Crawford, M. Avery, S. Sandholm, H. Fuelberg, Journal of Geophysical Research-Atmospheres 109 (2004) D15S07.

[2] K. Imrik, E. Farkas, G. Vasvári, I. Szilágyi, D. Sarzyński, S. Dóbé, T. Bérces, F. Márta, Physical Chemistry Chemical Physics 6 (2004) 3958.

[3] G. Kovács, J. Zádor, E. Farkas, R. Nádasdi, I. Szilágyi, S. Dóbé, T. Bérces, F. Márta, G. Lendvay, Physical Chemistry Chemical Physics 9 (2007) 4142.

[4] E. Delbos, P. Devolder, L. ElMaimouni, C. Fittschen, K. Brudnik, J. T. Jodkowski, E. Ratajczak, Physical Chemistry Chemical Physics 4 (2002) 2941.

[5] K.D. King, D.M. Golden, S.W. Benson, Journal of the American Chemical Society 92 (1970) 5541.

[6] M.J. Frisch et al., Gaussian 03, Revision D.01, Gaussian, Inc., Wallingford CT, 2004.

[7] K.J. Laidler, Theories of Chemical Reaction Rates, McGraw-Hill Book Company, New York, St. Louis, etc., 1969.

[8] K.H. Hoyermann, in Physical Chemistry –An Advanced Treatise, Vol VI B/Kinetics of Gas Reactions, Academic Press, New York, 1975.

[9] J.R. Alvarez-Idaboy, A. Galano, Theoretical Chemistry Accounts 126 (2010) 75.

[10] S.P. Sander, R.R. Friedl, J.R. Barker, D.M. Golden, M.J. Kurylo, P.H. Wine, J.P.D. Abbatt, J.B. Burkholder, C.E. Kolb, G.K. Moortgat, R.E. Huie, V.L. Orkin, Chemical Kinetics and Photochemical Data for Use in Atmospheric Studies, Evaluation Number 17, JPL Publication 10-6, Jet Propulsion Laboratory, Pasadena, 2011.

[11] K.D. King, D.M. Golden, S.W. Benson, Journal of Chemical Thermodynamics 3 (1971) 129.

[12] E.E. Greenwald, S.W. North, Y. Georgievskii, S. J. Klippenstein, Journal of Physical Chemistry A 109 (2005) 6031.

[13] J. Zádor, A.W. Jasper, J. A. Miller, Physical Chemistry Chemical Physics 11 (2009) 11040.

[14] J.T. Jodkowski, M.T. Rayez, J.C. Rayez, T. Bérces, S. Dóbé, Journal of Physical Chemistry A 102 (1998) 9219.

[15] E. Drougas, D.K. Papayannis, A.M. Kosmas, Journal of Molecular Structure-Theochem 623 (2003) 211.

[16] R.S. Timonen, J.A. Seetula, D. Gutman, Journal of Physical Chemistry 94 (1990) 3005.

[17] J. Espinosa-García, A. Márquez, S. Dóbé, Chemical Physics Letters 373 (2003) 350.

[18] A.M. El-Nahas, J.W. Bozzelli, J.M. Simmie, M.V. Navarro, G. Black, H.J. Curran, Journal of Physical Chemistry A 110 (2006) 13618.

[19] I. Szilágyi, K. Imrik, D. Sarzińsky, S. Dóbé, T. Bérces, Reaction Kinetics and Catalysis Letters 77 (2002) 341.

[20] J. Vázquez, M.E. Harding, J. Gauss, J.F. Stanton, Journal of Physical Chemistry A 113 (2009) 12447.

[21] R.S. Timonen, E. Ratajczak, D. Gutman, Journal of Physical Chemistry 92 (1988) 651.

[22] R.S. Timonen, J.A. Seetula, D. Gutman, Journal of Physical Chemistry 97 (1993) 8217.

[23] R.S. Timonen, J.A. Seetula, J.T. Niiranen, D. Gutman, Journal of Physical Chemistry 95 (1991) 4009.

[24] M.W. Chase, Journal of Physical Chemistry Reference Data Monogr. 9 (1998) 1.

[25] J. Chao, Journal of Physical Chemistry Reference Data 15 (1986) 1369.

[26] R. Janoschek, M.J. Rossi, International Journal of Chemical Kinetics 36 (2004) 661.

[27] D.J. Wuebbles, K.O. Patten, D. Wang, D. Youn, M. Martinez-Aviles, J.S.C. Francisco, Atmospheric Chemistry and Physics 11 (2011) 2371.

[28] A. Keil, P.B. Shepson, Journal of Geophysical Research-Atmospheres 111 (2006) D17303.

Supplementary data

Kinetics and mechanism of the reaction of acetonyl radical, $CH_3C(O)CH_2$, with Br_2

Gábor L. Zügner, Emese Szabó, Mária Farkas, Sándor Dóbé*

Institute of Materials and Environmental Chemistry, Research Centre for Natural Sciences, Hungarian Academy of Sciences, Pusztaszeri út 59-67, H-1025 Budapest, Hungary

Katarzyna Brudnik*, Dariusz Sarzyński, Jerzy T. Jodkowski[3]

Department of Physical Chemistry, Wroclaw Medical University, 50-140 Wroclaw, pl. Nankiera 1, Poland

Chemical Physics Letters**,** 568–569 (2013) 59–62

Table S1. Experimental conditions and results for the reaction $CH_3C(O)CH_2 + Br_2$ (1)

Table S2. G2 molecular parameters and energies for the reaction $CH_3C(O)CH_2 + Br_2$

Table S3 Cartesian coordinates optimized at the MP2/6-31G(d) level of theory

Table S4. Calculation of the rate coefficient k_1(TST)

*Corresponding authors. *E-mail*: dobe.sandor@ttk.mta.hu (S.D.); katarzyna.brudnik@umed.wroc.pl (K.B.).

[3]Deceased.

Table S1. Experimental conditions and results for the reaction $CH_3C(O)CH_2 + Br_2$ (1)

T **(K)**	***P*** **(mbar)**	***w*** **(cm s^{-1})**	**10^{-13} [Br_2] (molecule cm^{-3})**	k_1' **(s^{-1})**	k_1' **error (2σ) (s^{-1})**
298 ± 3	3.5 ± 0.6	1070	0.51	19.85	3.42
			0.89	25.87	2.34
			1.01	37.22	2.34
			1.91	49.29	2.94
			2.50	64.01	3.66
			2.85	82.94	6.08
			3.54	84.44	5.18
			3.89	104.41	16.48
			4.86	105.37	3.22
			5.57	133.73	2.36
			6.50	151.31	4.44
			6.96	190.08	11.14
			9.41	245.93	6.88
			11.90	279.08	19.42
k_1(298 K) = (2.33 ± 0.04 (2 σ)) × 10^{-12} cm^3 $molecule^{-1}$ s^{-1}					
322 ± 2	3.5 ± 0.6	1230	0.25	11,5	1.26
			0.41	17.3	1.40
			2.76	70.82	2.48
			2.62	79.1	3.68
			5.29	144.5	4.38
			8.08	198.5	10.02
			7.80	199.4	14.18
			8.70	232.9	12.10
k_1(322 K) = (2.53 ± 0.16 (2σ)) × 10^{-12} cm^3 $molecule^{-1}$ s^{-1}					
361 ± 2	3.4 ± 0.2	1300	0.42	12.4	0.92
			1.30	47.1	1.88
			1.75	53.9	4.72
			3.05	85.0	3.14
			4.22	110.3	5.74
			5.46	145.7	4.24
			6.50	184.8	9.74
k_1(361 K) = (2.73 ± 0.06 (2σ)) × 10^{-12} cm^3 $molecule^{-1}$ s^{-1}					

Table S2. G2 molecular parameters and energies for the reaction $CH_3C(O)CH_2 + Br_2$[a,d]

Geometry	$CH_2C(O)CH_3$	$Br–Br...CH_2C(O)CH_3$[b] (MC)	$Br...Br...CH_3C(O)CH_2$[c] (TS)	$BrCH_2C(O)CH_3$
C_1C_2	1.4772	1.4774	1.5097	1.5204
C_2C_3	1.5153	1.5148	1.5088	1.5082
C_1H_1	1.0820	1.0823	1.0850	1.0885
C_1H_2	1.0832	1.0823	1.0859	1.0923
C_3H_3	1.0891	1.0893	1.0893	1.0903
C_3H_4	1.0944	1.0942	1.0927	1.0934
C_3H_5	1.0944	1.0938	1.0951	1.0938
C_2O_1	1.2036	1.2043	1.1970	1.2264
C_1Br_1		3.9136	2.4556	1.9607
H_1Br_1		3.3600	5.04916	
Br_1Br_2		2.3119	2.3568	
$C_1C_2C_3$	115.9810	115.8834	115.9281	117.9551
$H_1C_1C_2$	118.0945	118.0196	115.8825	109.6724
$H_2C_1C_2$	122.2960	122.0804	120.0511	111.2951
$H_3C_3C_2$	109.0617	109.1282	109.1348	108.8209
$H_4C_3C_2$	110.0423	109.1865	110.0255	109.7481
$H_5C_3C_2$	110.0423	110.6258	109.2712	111.1079
$C_1C_2O_1$	121.2640	121.3250	119.7849	119.1058
$Br_1C_1C_2$		89.9652	99.9025	110.9375
$H_1Br_1Br_2$		78.0454	152.9579	
$H_1C_1C_2C_3$	0.0000	–178.1289	–176.0337	–173.0781
$H_2C_1C_2C_3$	180.0000	3.1015	31.0273	63.7299
$H_1C_1C_2O_1$	180.0000	1.1886	4.9883	–115.0418
$H_3C_3C_2C_1$	180.0000	–175.0563	176.0337	–164.1345
$H_4C_3C_2C_1$	59.1559	64.5108	54.3915	76.1810
$H_5C_3C_2C_1$	-59.1559	–53.1652	–63,8556	–42.3487
$Br_1C_1C_2C_3$		–1.5336	–76.1413	–54.4129
***B*:**	10.81742	1.88749	4.34337	7.40345
	9.15151	0.59472	0.52982	1.59590
	5.1151	0.49924	0.50881	1.41641

[a] Geometries have been optimized at the MP2/6-31G(d) level of theory; the bond lengths are given in Å, valence and dihedral angles in degrees. The SCF/6-31G(d) vibrational frequencies are scaled by 0.8929 and are given in cm^{-1} . The rotational constants, *B*, have been obtained using MP2/6-31G(d) optimization and are given in GHz. The total G2-energies, E_0(G2), refer to 0 K and are given in Hartrees.

[b] Pre-reaction complex.

[c] Transition state structure.

[d] The G2-molecular parameters for the other molecules are the following: Br: E_0(G2) = –2572.5329449 a.u., Br_2: *R*(Br–Br) = 2.3128 Å, □₁ = 323 cm^{-1} , and E_0(G2)= –5337.302908 a.u.

Table S2 (continued)

Frequency	$CH_2C(O)CH_3$	Br–Br...$CH_2C(O)CH_3$[b] (MC)	Br...Br...$CH_3C(O)CH_2$[c] (TS)	$BrCH_2C(O)CH_3$
1	55	6	254***i***	50
2	364	30	36	100
3	403	40	41	173
4	487	54	79	357
5	501	62	90	441
6	676	100	99	524
7	790	323	174	642
8	901	383	357	761
9	1010	436	497	834
10	1026	491	523	984
11	1209	505	584	1016
12	1374	714	776	1129
13	1393	789	832	1206
14	1448	930	896	1391
15	1451	1012	1022	1389
16	1453	1041	1042	1434
17	2865	1194	1192	1438
18	2914	1359	1389	1450
19	2962	1397	1416	1808
20	2982	1454	1445	2879
21	3080	1456	1448	2936
22		1459	1480	2945
23		2870	2870	2972
24		2929.	2924	3028
25		2958	2971	
26		2990	2990	
27		3087	3091	
E_0(G2):	**–192.1595753**	**–5337.3029080**	**–5337.3004814**	**–2764.7958441**

[a] Geometries have been optimized at the MP2/6-31G(d) level of theory; the bond lengths are given in Å, valence and dihedral angles in degrees. The SCF/6-31G(d) vibrational frequencies are scaled by 0.8929 and are given in cm^{-1} . The rotational constants, *B*, have been obtained using MP2/6-31G(d) optimization and are given in GHz. The total G2-energies, E_0(G2), refer to 0 K and are given in Hartrees.

[b] Pre-reaction complex.

[c] Transition state structure.

[d] The G2-molecular parameters for the other molecules are the following: Br: E_0(G2)= –2572.5329449 a.u., Br_2: *R*(Br–Br) = 2.3128 Å, □₁ = 323 cm^{-1} , and E_0(G2)= –5337.302908 a.u.

Table S3 Cartesian coordinates optimized at the MP2/6-31G(d) level of theory [a].

No.	Atom	$CH_2C(O)CH_3$			$Br–Br...CH_2C(O)CH_3$ (MC)			$Br...Br..CH_3C(O)CH_2$ (TS)			$BrCH_2C(O)CH_3$		
		X	Y	Z	X	Y	Z	X	Y	Z	X	Y	Z
1	C_1	-0.16114	0.00000	-1.42969	0.57705	-1.50317	0.57658	0.84597	-1.53495	0.33196	1.46544	-1.94327	0.07256
2	C_2	-0.16114	0.00000	0.04748	-0.84313	-1.84268	0.35180	-0.56608	-1.26163	-0.12686	0.23501	-2.63150	-0.49657
3	C_3	1.20105	0.00000	0.71131	-1.83571	-0.72215	0.58409	-1.64936	-1.49409	0.89735	-1.1197	-2.12024	-0.07471
4	H_1	0.75447	0.00000	-2.00842	0.88556	-0.52970	0.93523	-0.76765	-0.90943	-1.25295	0.38149	-3.58469	-1.25425
5	H_2	-1.11565	0.00000	-1.93922	1.31852	-2.26934	0.39081	-2.60905	-1.19812	0.47548	-1.87205	-2.86803	-0.32688
6	O_1	-1.18995	0.00000	0.67212	-1.17455	-2.94364	-0.00645	-1.43453	-0.92489	1.805013	-1.34321	-1.18832	-0.60109
7	H_3	1.06984	0.00000	1.79252	-2.84676	-1.11239	0.47408	-1.67257	-2.55591	1.16429	-1.14230	-1.90237	0.99698
8	H_4	1.76914	0.88272	0.40176	-1.65741	0.07325	-0.14585	1.62874	-1.31042	-0.38497	2.35970	-2.33364	-0.40984
9	H_5	1.76914	-0.88272	0.40176	-1.69797	-0.28513	1.57729	1.03699	-2.30197	1.07646	1.52160	-2.06389	1.15675
10	Br_1				0.32478	2.26709	1.73968	1.25289	0.44757	1.72251	1.40697	-0.01260	-0.26405
11	Br_2				0.21157	2.40001	-0.56557	1.41437	2.24586	3.23732			

[a] The coordinates are given in Angstroms; R(Br–Br) = 2.3128 Å

Table S4

Calculation of the rate coefficient k_1(TST)

T (K)	Kc (cm,molec)	s	s(kT/h)Kc (cm,molec,s)	tunn.*) corr.	k_1(TST) (cm,molec,s)
100.	5.052E-27	2	2.105E-14	1.697	3.573E-14
200.	1.196E-26	2	9.968E-14	1.174	1.170E-13
250.	1.588E-26	2	1.654E-13	1.112	1.838E-13
298.	1.982E-26	2	2.463E-13	1.078	2.656E-13
300.	1.998E-26	2	2.498E-13	1.077	2.691E-13
350.	2.424E-26	2	3.535E-13	1.057	3.736E-13
400.	2.863E-26	2	4.773E-13	1.044	4.981E-13
450.	3.317E-26	2	6.220E-13	1.034	6.434E-13
500.	3.785E-26	2	7.886E-13	1.028	8.106E-13
600.	4.759E-26	2	1.190E-12	1.019	1.213E-12
700.	5.786E-26	2	1.688E-12	1.014	1.712E-12
800.	6.865E-26	2	2.289E-12	1.011	2.314E-12
900.	7.994E-26	2	2.998E-12	1.009	3.024E-12
1000.	9.171E-26	2	3.822E-12	1.007	3.849E-12
1500.	1.573E-25	2	9.831E-12	1.003	9.861E-12
2000.	2.330E-25	2	1.942E-11	1.002	1.945E-11
2500.	3.176E-25	2	3.309E-11	1.001	3.313E-11
3000.	4.104E-25	2	5.131E-11	1.001	5.135E-11

*) Wigner tunneling correction for 284i